

# Palmitic acid acutely stimulates glucose uptake via activation of Akt and ERK1/2 in skeletal muscle cells<sup>S</sup>

Jing Pu,<sup>\*,†</sup> Gong Peng,<sup>\*,†</sup> Linghai Li,<sup>\*</sup> Huimin Na,<sup>\*</sup> Yanbo Liu,<sup>\*,§</sup> and Pingsheng Liu<sup>1,\*</sup>

National Laboratory of Biomacromolecules, Institute of Biophysics,<sup>\*</sup> Graduate University,<sup>†</sup> Chinese Academy of Sciences, Beijing, 100101, China; and College of Life Science,<sup>§</sup> Guizhou University, Guiyang, Guizhou, China

**Abstract** Chronic exposure to saturated fatty acids can cause insulin resistance. However, the acute effects of fatty acids are not clear and need to be elucidated because plasma fatty acid concentrations fluctuate postprandially. Here, we present the acute effects of palmitate (PA) on skeletal muscle cells and their underlying molecular mechanisms. Immunofluorescence results showed that PA rapidly induced GLUT4 translocation and stimulated glucose uptake in rat skeletal muscle cell line L6. Phosphorylation of AMP-activated protein kinase (AMPK), Akt, and extracellular signal-related kinase1/2 (ERK1/2) was enhanced by PA in a time-dependent manner. Cell surface-bound PA was sufficient to stimulate Akt phosphorylation. The inhibitors of PI3 kinase (PI3K), AMPK, Akt, and ERK1/2 could decrease PA-induced glucose uptake, and PI3K inhibitor decreased AMPK, Akt, and ERK1/2 phosphorylation. Weakening AMPK activity reduced phosphorylation of Akt but not ERK1/2, and Akt inhibitor could not affect ERK1/2 activation either. Meanwhile, ERK1/2 inhibitors had no effect on Akt phosphorylation. Taken together, our data suggest that PA-mediated glucose uptake in skeletal muscle cells may be stimulated by the binding of PA to cell surface and followed by PI3K/AMPK/Akt and PI3K/ERK1/2 pathways independently.—Pu, J., G. Peng, L. Li, H. Na, Y. Liu, and P. Liu. Palmitic acid acutely stimulates glucose uptake via activation of Akt and ERK1/2 in skeletal muscle cells. *J. Lipid Res.* 2011. 52: 1319–1327.

**Supplementary key words** fatty acid • GLUT4 • phosphorylation • extracellular signal-related kinase • PI3 kinase

Plasma fatty acid concentrations are much higher in patients with type 2 diabetes than in healthy subjects. Previous studies have shown that chronically elevated fatty acids can cause the body to be unresponsive to insulin and in turn reduces insulin-stimulated glucose uptake (1, 2). Of the tissues and organs that respond to insulin stimulation,

skeletal muscle consumes more than 70% of the plasma glucose, suggesting that whole body plasma glucose concentration is tightly associated to the sensitivity of muscle tissue to insulin (3, 4). Muscle cells ingest fatty acids from the blood and store them as intramyocellular triglycerides (IMTGs) in a cellular organelle lipid droplet (5, 6). Mounting evidence indicates that chronically elevated fatty acids in the plasma induce excess storage of IMTG, which in turn plays a key role in the development of insulin resistance (7–9). Furthermore, Manco et al. (8) have suggested that, in addition to IMTG concentration, the IMTG fatty acid fraction pattern, i.e., whether palmitic acid is present rather than oleic acid, is significantly correlated to glucose uptake in muscle tissue. This is consistent with other reports suggesting that saturated fatty acids suppress body insulin sensitivity.

During fasting, adipocytes release stored lipids as free fatty acids into the blood to provide an energy source in the animal body. As a result, the concentrations of fatty acids in the blood are not consistent. In fact, fatty acid concentrations vary widely from hour to hour and display waves according to nutritional state and the presence of regulators including hormones, as well as metabolic and neural signals (10, 11). Although a few studies have reported the acute effects of fatty acids, conclusions concerning how energy-consuming tissues, such as skeletal muscle, respond to acute rises in fatty acid levels have been inconsistent and the underlying molecular mechanisms controlling these responses are still unclear. For example,  $\alpha$ -lipoic acid has been shown to enhance basal glucose uptake both in normal and *ob/ob* mice (12),

Abbreviations: AMPK, AMP-activated protein kinase; AMPK-DN, AMPK dominant negative; ERK1/2, extracellular signal-related kinase; IMTG, intramyocellular triglyceride; KRBH, Krebs-Ringer HEPES buffer; MEK, MAPK/ERK kinase; N.C., negative control; PA, palmitic acid or palmitate; p-Akt, phosphorylated Akt; p-AMPK, phosphorylated AMPK; PI3K, PI3 kinase; siAkt, short interference RNA targeting Akt; siRNA, short interference RNA.

<sup>1</sup>To whom correspondence should be addressed.

e-mail: pliu@ibp.ac.cn

<sup>S</sup>The online version of this article (available at <http://www.jlr.org>) contains supplementary data in the form of one figure.

This work was supported by grants from the Ministry of Science and Technology of China (2006CB911001 and 2009CB919003) and the National Natural Science Foundation of China (30871229).

Manuscript received 18 November 2010 and in revised form 9 March 2011.

Published, JLR Papers in Press, April 25, 2011

DOI 10.1194/jlr.M011254

Copyright © 2011 by the American Society for Biochemistry and Molecular Biology, Inc.

This article is available online at <http://www.jlr.org>

whereas palmitic acid (PA) treatment was reported to inhibit insulin-stimulated but not basal glucose uptake (13).

To elucidate the mechanism underlying the response of skeletal muscle to acute increases in fatty acids, we examined the acute effects of PA on glucose uptake and on phosphorylation of AMP-activated protein kinase (AMPK), Akt, and extracellular signal-related kinase (ERK) 1/2 in skeletal cell lines. We found that PA stimulated GLUT4 translocation to the plasma membrane and glucose uptake enhancement. Our data also suggest that PI3 kinase (PI3K), AMPK, Akt, and ERK1/2 play critical roles in PA-induced glucose uptake and that cell surface-bound PA is sufficient to trigger the signal transduction.

## MATERIALS AND METHODS

### Materials

Sodium PA, insulin, myc polyclonal antibody, fatty acid-free BSA, 5-aminoimidazole-4 carboxamide 1- $\beta$ -D-ribofuranoside (AICAR), Compound C, API-2, Lipid Standard, and 2-deoxy-D-glucose were purchased from Sigma-Aldrich (St. Louis, MO). 2-Deoxy-D-[ $^3$ H]glucose and TLC plates were obtained from GE Healthcare (UK). Antibodies against phosphorylated Akt (Ser 473), total Akt, phosphorylated AMPK (Thr172), phosphorylated ERK1/2 (p44/42 MAPK) (Thr202/Tyr204), and GAPDH were from Cell Signaling Technology (Beverly, MA). Myc monoclonal antibody was purchased from Upstate (Billerica, MA).  $^3$ H-PA was from PerkinElmer Life Sciences (Waltham, MA). LY294002 and API-2 were from Biomol (Plymouth Meeting, PA). PD98058 and U0126 were from Beyotime Institute of Biotechnology (Haimen, China). Short interference RNA (siRNA) duplex targeting Akt (siAkt) and AMPK and negative control siRNA were from GenePharma (Shanghai, China). The L6-GLUT4 $^{myc}$  (L6) cell line, a rat skeletal muscle cell line which stably over-expresses GLUT4, was obtained from Dr. Amira Klip, Division of Cell Biology, Hospital for Sick Children, Toronto, Canada. The myc-tagged AMPK dominant negative mutant constructed into pcDNA3.1 was a kind gift from Dr. David Carling, Cellular Stress Group, MRC Clinical Sciences Centre, London, UK.

### Cell culture

L6-GLUT4 $^{myc}$  cells were maintained in  $\alpha$ -minimal essential medium ( $\alpha$ -MEM) supplemented with 10% (v/v) FBS, 2  $\mu$ g/ml blasticidin S, 100 units/ml penicillin, and 100 units/ml streptomycin at 37°C with 5% CO<sub>2</sub>. L6 cells were differentiated into myotubes within 7 days in medium supplemented with 2% FBS. Mouse C2C12 myoblasts (American Type Culture Collection) were maintained in DMEM supplemented with 10% (v/v) FBS, 100 units/ml penicillin, and 100 units/ml streptomycin at 37°C with 5% CO<sub>2</sub>.

### Palmitate preparation and treatment

Sodium palmitate was prepared according to our previously published method (14). Briefly, sodium palmitate was added to ethanol to a final concentration of 100 mM and sonicated on ice at 200 W using 10 s on, 3 s off pulses until the mixture became a milky homogenous solution. The PA stock solution was added to growth medium containing 10% FBS at 60°C and the medium was cooled to 37°C for cell treatment unless otherwise stated. For the control, the same amount of ethanol was added to the growth medium containing 10% FBS as a vehicle.

### Cell transfection

The sequence of the siAkt was that given by Katome et al. (15), and AMPK  $\alpha$  by Konrad et al. (16). L6 cells were nucleofected with siRNA or plasmids following the manufacturer's procedure. After 48 h, or the times indicated, the analysis was performed.

### Detection of cell surface GLUT4 by immunofluorescence

Immunofluorescence was used to detect GLUT4 on the cell surface using a previously published method with slight modifications (17). L6-GLUT4 $^{myc}$  cells were seeded on a glass-bottomed plate overnight. After treatment with PA or insulin, cells were immediately placed on ice and washed three times with ice-cold Krebs-Ringer HEPES buffer (KRBH) (120 mM NaCl, 25 mM HEPES, 4.6 mM KCl, 1 mM MgSO<sub>4</sub>, 1.2 mM KH<sub>2</sub>PO<sub>4</sub>, and 1.9 mM CaCl<sub>2</sub>, pH 7.4). After blocking with 5% goat serum in KRBH at 4°C for 10 min, cells were incubated with 2.5 mg/ml anti-myc polyclonal antibody at 4°C for 1 h, washed with ice-cold KRBH, fixed in 3% formaldehyde (PFA) at 4°C for 20 min, and then incubated with 50 mM NH<sub>4</sub>Cl for another 10 min. After washing with KRBH, cells were incubated with fluorescein isothiocyanate (FITC)-conjugated goat anti-rabbit IgG (1:500 dilution) for 45 min at 4°C, washed with ice-cold KRBH, and then examined immediately in KRBH with an Olympus FV500 confocal fluorescence microscope.

### Measurement of 2-deoxy-D-[ $^3$ H]glucose uptake

L6-GLUT4 $^{myc}$  cells were treated with PA, washed three times with prewarmed KRBH, and incubated in KRBH containing 0.5  $\mu$ Ci/ml 2-deoxy-D-[ $^3$ H]glucose and 50  $\mu$ M 2-deoxy-glucose at 37°C for 5 min. Cells were then washed three times with ice-cold KRBH and then lysed with 1% SDS. Radioactivity was measured using a Perkin-Elmer scintillation counter. Each experiment was performed three times at least with triplicate independently.

### Protein preparation and Western blotting

After the treatments indicated, cells were lysed directly with 2 $\times$ SDS sample buffer and sonicated twice (7 s each time) at 200 W. Rat tissue samples were prepared according to a previously published method (18). Briefly, 50–70 mg wet tissues were sonicated in 2 $\times$ SDS sample buffer to dissolve cellular protein, and total protein was precipitated using 7.2% TCA. Protein pellets were washed with acetone and dissolved in 2 $\times$ SDS sample buffer by sonication. Total proteins were resolved by 10% SDS-PAGE, transferred to a polyvinylidene fluoride membrane, blotted using the antibodies indicated, and detected using ECL.

### Palmitate treatment of rat skeletal muscle

Male Sprague-Dawley rats (200–250 g) were anesthetized intraperitoneally with chloral hydrate (10%, 1 ml/200 g body weight) and subjected to transcardiac perfusion with 20 ml 2 mM PA in saline containing 10% FBS. The success of perfusion was confirmed by loss of color in the liver. After perfusion, the soleus muscle strips were isolated, incubated in 2 mM PA in saline containing 10% FBS at 37°C for the times indicated, immediately frozen in liquid nitrogen, and stored at –80°C until required. All animal experiments were approved by the Institutional Animal Care and Use Committee and followed the Animal Use Guidelines of the Institute of Biophysics, Chinese Academy of Sciences.

### Lipid extraction and TLC

The cells were lysed with 1% triton X-100 after treatment with  $^3$ H-labeled PA and total lipids were extracted with lipid extract reagent (chloroform-methanol-acetic acid = 50:50:1, by vol) for TLC. Chromatograms were developed with the developing solvent of

N-hexane-diethyl ether-acetic acid (80:20:1, by vol), and then the TLC plates were stained in iodine vapor after being air-dried at room temperature for 20 min. The silica gel of the plates was scraped following the separated lipid bands from Lipid Standard and subjected to scintillation counting using a Perkin-Elmer scintillation counter.

### Statistical analyses

Statistical analyses were performed using Microsoft Office Excel 2007 and OriginPro 7.5. Differences among relevant groups were assessed using unpaired Student's *t*-tests. *P* < 0.05 was considered significant. Values presented are means ± SD.

## RESULTS

### Palmitate stimulates GLUT4 translocation and basal glucose uptake

To determine the acute effect of PA on glucose uptake in skeletal muscle, a rat skeletal muscle cell line that stably

expresses GLUT4 with a myc tag located in its first exofacial loop, L6-GLUT4<sup>myc</sup> (L6), was treated with 300 μM PA or 100 nM insulin. As shown in Fig. 1A, insulin increased plasma membrane-localized GLUT4 as expected. Surprisingly, PA treatment also stimulated GLUT4 translocation to the plasma membrane. We then measured glucose uptake in L6 cells treated with PA. Uptake of <sup>3</sup>H-labeled 2-deoxy-glucose in L6 cells was increased by 28% (*P* < 0.05), 69% (*P* < 0.001), 76% (*P* < 0.001), 93% (*P* < 0.001), 86% (*P* < 0.001), and 85% (*P* < 0.001) after 5, 10, 15, 20, 30, and 60 min of treatment with 300 μM PA, respectively (Fig. 1B). The increased glucose uptake in skeletal muscle cells acutely exposed to PA correlated with the localization of GLUT4 on the plasma membrane.

### Palmitate stimulates phosphorylation of Akt, AMPK, and ERK1/2

Because the stimulatory effect of PA on GLUT4 translocation and glucose uptake was similar to that of insulin, we

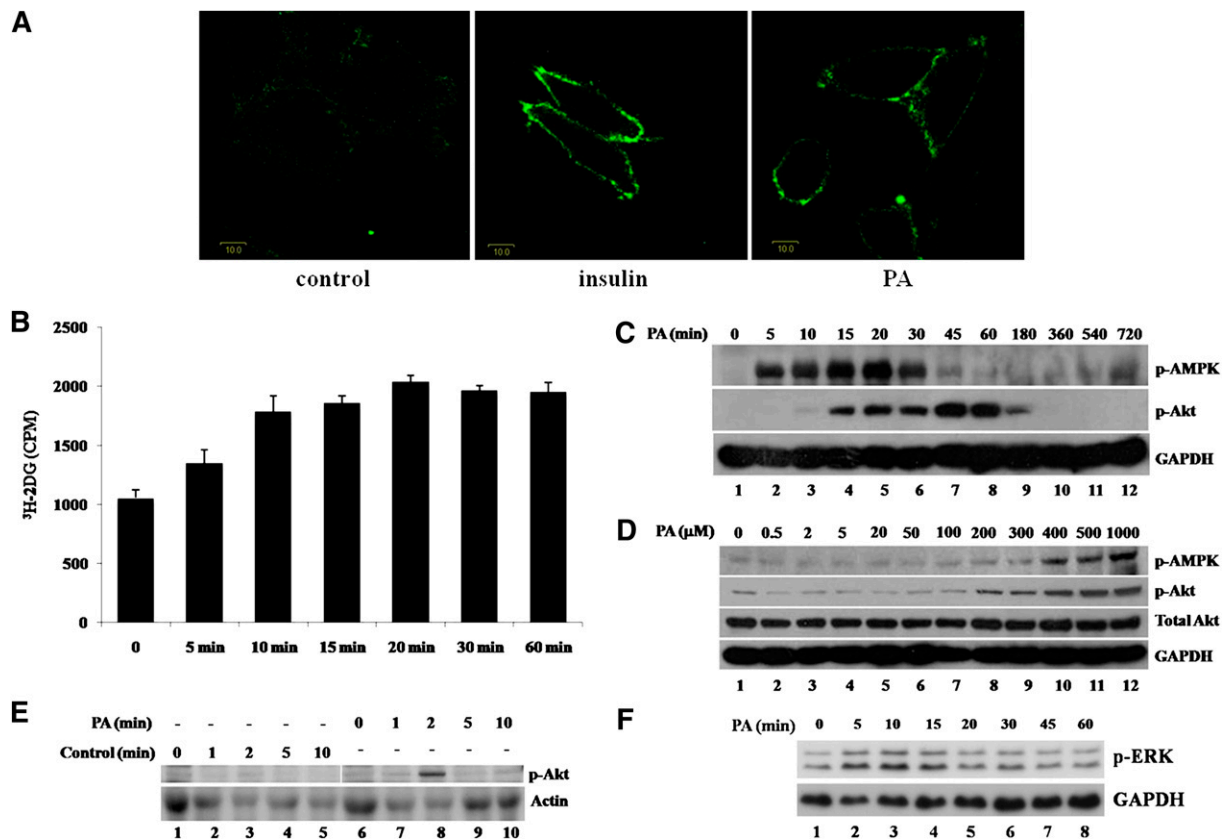


**Fig. 1.** Palmitate stimulates GLUT4 translocation, glucose uptake, and phosphorylation of AMPK, Akt, and ERK. **A:** L6-GLUT4<sup>myc</sup> (L6) cells were treated with (right panel) or without (left panel) PA (300 μM) for 30 min or 100 nM insulin (middle panel) for 20 min and washed three times with ice-cold KRBH buffer. Immunofluorescence was performed with anti-myc polyclonal antibody and FITC-conjugated IgG. Fluorescence images were obtained with an Olympus FV500 confocal fluorescence microscope. Bar = 10 μm. **B:** L6 cells were treated with or without 300 μM PA for the indicated times. Cells were then treated with <sup>3</sup>H-labeled 2-deoxy-D-glucose and glucose uptake was assayed. Data are presented as means ± SD (*n* = 3) from one of four time-independent experiments with triplicate. **C, D:** L6 myoblasts were incubated in the presence of 300 μM PA for the times indicated (**C**) or with the indicated concentrations of PA for 30 min (**D**). Cells were lysed in 2× SDS sample buffer and total protein was subjected to Western blotting using the antibodies indicated. GAPDH was included as an internal control. **E:** A total of 2 mM palmitate in saline containing 10% FBS was used to perfuse male Sprague-Dawley rats. After perfusion, isolated soleus muscle strips were incubated in 2 mM palmitate at 37°C for the times indicated. Control rats were treated with 10% FBS-containing saline. The cost times for each step are indicated in supplementary Fig. 1E. Western blots representing one of three experiments are shown. **F:** L6 cells were treated as in **C** for the indicated times and whole cell lysates were subjected to Western blotting.

examined the activation of Akt, a key protein involved in insulin-stimulated GLUT4 translocation. Akt phosphorylation (Ser 473) was stimulated by PA in a time- and dose-dependent manner (Fig. 1C–E and supplementary Fig. 1A). Interestingly, activation of Akt in L6 myoblasts was observed after 10 min and peaked at 45 min, then decreased dramatically after 1 h, and became nondetectable after 3 h (Fig. 1C), suggesting that a signal transduction cascade initiated by PA leads to the activation of Akt. In addition, PA also could stimulate Akt activation in differentiated L6 myotubes but made a shorter duration of Akt activation compared with L6 myoblasts (supplementary Fig. 1A). To verify the stimulatory effect of PA on Akt activation, we carried out similar experiments using mouse skeletal muscle cell line C2C12, and, as a result, PA also activated Akt rapidly (Fig. 2A, lanes 1 to 5). Further verification was carried out using rat skeletal muscle. After anesthetization, rats were perfused with 2 mM PA. Skeletal muscle strips were collected and then incubated *in vitro* with 2 mM PA (Fig. 1E and supplementary Fig. 1F). Similar to the results obtained from experiments using cell lines, PA stimulated Akt phosphorylation in rat skeletal muscle tissue (Fig. 1E, lane 8). Together, these data suggest that this acute response of PA may be physiologically relevant because results were similar for mouse and rat skeletal muscle cell lines as well as rat skeletal muscle tissue. We then investigated this putative PA-mediated signaling pathway in more detail. Previous studies have shown that chronic treatment with PA can induce AMPK phosphorylation (19, 20) and that AMPK is able to induce Akt activation (21). Therefore, we tested whether AMPK can also be activated by PA treatment. Our data show that short-term treatment with PA is also able to stimulate AMPK phosphorylation (Thr172) starting as early as 5 min and reaching a peak at 20 min. After 1 h, the signal could not be detected (Fig. 1C). As AMPK activation takes place more rapidly than Akt activation, it is possible that AMPK may mediate PA-induced Akt activation. In addition, phosphorylation of AMPK and Akt was stimulated by PA in a dose-dependent manner (Fig. 1D). Besides PA, we also examined the acute effects of other plasma-abundant fatty acids on skeletal muscle cells. Interestingly, linoleic acid, oleic acid, and stearic acid all could acutely stimulate Akt and AMPK phosphorylation in a dose-dependent manner in L6 cells (supplementary Fig. 1B, C, and D). Furthermore, the combination of PA, linoleic acid, oleic acid, and stearic acid had similar effects (supplementary Fig. 1E), of which ratio mimicked the fatty acid concentration ratio in rat plasma (22).

During PA short-term treatment, besides AMPK and Akt, ERK1/2 was also stimulated. The Western blot results showed that phosphorylation of both p44 (Thr202) and p42 (Tyr204) was increased after 5 min and returned to basal level after 15 min (Fig. 1F). ERK1/2 stimulation implied that it might participate PA-induced glucose uptake.

### Cell surface-bound palmitate stimulates Akt phosphorylation

Acute responses of rat skeletal muscle cells to PA (activation of AMPK, Akt, ERK1/2, and stimulation of glucose

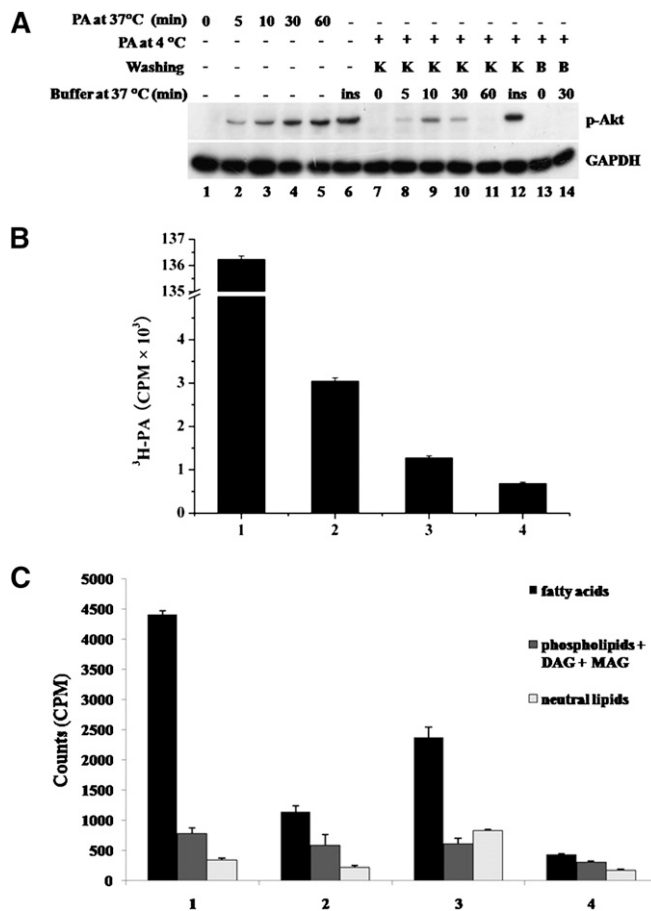


**Fig. 2.** Binding of palmitate to the plasma membrane is required for stimulation of Akt phosphorylation. A: C2C12 mouse muscle cells were treated with 300  $\mu$ M PA (lanes 2 to 5) for the times indicated or 100 nM insulin (lane 6) for 20 min. By way of comparison, C2C12 cells were incubated in the presence of 300  $\mu$ M PA at 4°C for 1 h and then washed three times with ice-cold KRBH buffer or 0.4% fatty acid-free BSA solution. After washing, cells were either lysed with 2 $\times$ SDS sample buffer (lane 7 and lane 13) or incubated in prewarmed KRBH buffer at 37°C for the times indicated (lanes 8 to 11, lane 14). A total of 100 nM insulin in prewarmed KRBH buffer was used to treat cells at 37°C for 20 min (lane 12) as a positive control. After incubation, cells were lysed and total protein was subjected to Western blotting using the antibodies indicated. GAPDH was included as an internal control. K, KRBH; B, BSA; ins, insulin. B: Cells were treated with 300  $\mu$ M PA plus 0.2  $\mu$ Ci/ml <sup>3</sup>H-labeled PA at 4°C for 1 h and washed three times with ice-cold KRBH buffer or 0.4% fatty acid-free BSA solution. Cells were then lysed and radio-labeled lipids were measured by scintillation counting. Data are presented as means  $\pm$  SD (n = 3). Bar 1: total input. Bar 2: <sup>3</sup>H labeled lipids remaining prior to washing. Bar 3: <sup>3</sup>H labeled lipids remaining after washing with KRBH. Bar 4: <sup>3</sup>H labeled lipids remaining after washing with BSA. Effective binding amount = (Bar 3–Bar 4)/Bar 1 = 0.43% of total input. C: The same experiments were carried out as in B and then cells were incubated at 37°C for 10 min. Then the cells were lysed, and the total lipids were extracted and separated by TLC. <sup>3</sup>H-labeled lipids were measured by scintillation counting. Data are presented as means  $\pm$  SD (n = 3) from one of three time-independent experiments with triplicate. Group 1: lipids from the cells that were washed by KRBH buffer at 4°C. Group 2: lipids from the cells that were washed by BSA solution at 4°C. Group 3: lipids from the cells that were washed by KRBH at 4°C and then incubated at 37°C for 10 min. Group 4: lipids from the cells that were washed by BSA solution at 4°C and then incubated at 37°C for 10 min.

uptake) indicate that PA may function as a soluble factor that can stimulate skeletal muscle cells by binding to the surface membrane in order to transduce its signal. To test this hypothesis, PA binding to mouse skeletal muscle C2C12 cells was achieved by incubating cells with PA for 1 h at 4°C to avoid PA internalization. Cells were then washed with ice-cold KRBH to remove unbound PA and transferred to 37°C to activate signal transduction. Akt phosphorylation appeared after 5 min (Fig. 2A, lane 8), reached a maximum at 10 min (lane 9), and declined thereafter, similar to the time-dependent manner of Akt activation at 37°C. However, when 0.4% fatty acid-free BSA-containing KRBH was used to wash the cells, Akt phosphorylation could not be detected (lane 14), suggesting that binding of PA to the cell surface is necessary for acute Akt stimulation. We conducted the same experiment with trace amounts of <sup>3</sup>H-labeled PA and found that the effective amount of PA was as little as 0.43% of the original amount of PA applied (Fig. 2B). To investigate the metabolism of PA during the PA treatment, the total lipids were extracted and separated by TLC. The data showed that fatty acid is the majority (79.8% ± 1.1%) of the total lipids from the cells after washing by KRBH buffer at 4°C (Fig. 2C, group 1) and still the main composition (62.4% ± 4.6%) after 10 min incubation at 37°C (Fig. 2C, group 3). The content of PA was significant different between KRBH washing and BSA washing, whereas phospholipids, monoacylglycerol, diacylglycerol, and triglyceride did not change significantly (Fig. 2C, group 1 vs. group 2). These data indicate that PA is the factor to induce Akt activation.

### Activation of Akt is involved in palmitate-stimulated glucose uptake

The above experiments showed that PA could acutely stimulate glucose uptake and Akt activity, suggesting that Akt may be involved in PA-induced glucose uptake. We applied an Akt selective inhibitor API-2 (23) to block Akt activity. As a result, API-2 could abolish Akt phosphorylation (Fig. 3A) as well as decrease PA-induced glucose uptake significantly (Fig. 3B). In addition, Akt expression was reduced by RNA interference to verify the results from experiments using inhibitor. siRNA duplexes were nucleofected into L6 cells and total Akt expression levels were determined at 24, 48, and 72 h after nucleofection. Compared with negative control siRNA (N.C.), siAkt could efficiently downregulate Akt expression (Fig. 3C). As Fig. 3D shows, in further analyses performed at 48 h after nucleofection, siAkt transfection decreased PA-induced glucose uptake, whereas N.C. transfection did not. Together, these data suggest that PA-triggered signal transduction induces glucose uptake in skeletal muscle cells via Akt activation.

### Activation of AMPK is involved in palmitate-stimulated Akt phosphorylation and glucose uptake

Because AMPK and Akt activation was observed sequentially in PA-treated cells (Fig. 1C), we studied the relationship between AMPK and Akt and the role of AMPK in PA-induced glucose uptake. AMPK agonist AICAR was used to stimulate AMPK phosphorylation in L6 cells, and the Western blots showed that not only

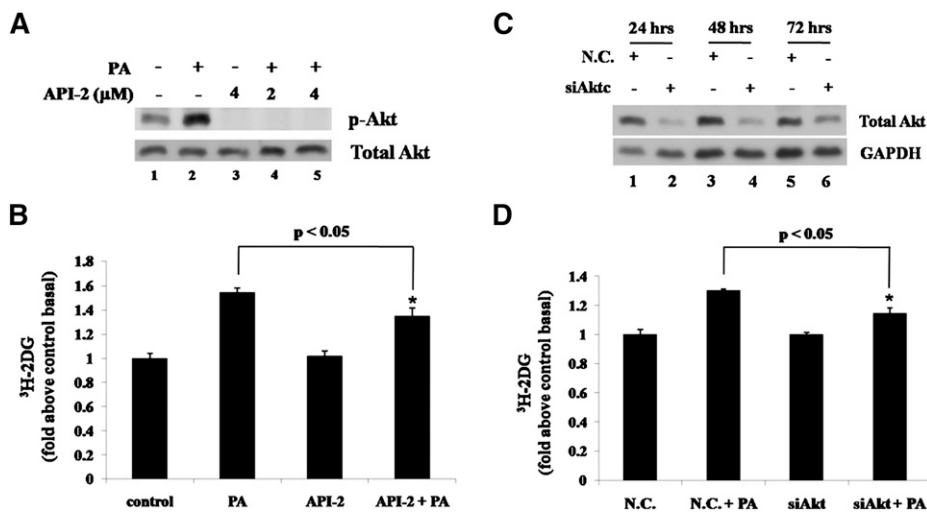


**Fig. 3.** Akt is involved in palmitate-stimulated glucose uptake. A: L6 cells were pretreated with or without API-2 at indicated concentrations for 30 min and then with or without 300 μM PA alone or with inhibitor for 30 min, and total cell lysates were subjected to Western blotting. B: L6 cells were treated with 2 μM API-2 and 300 μM PA as in A and then <sup>3</sup>H-labeled 2-deoxy-D-glucose uptake assays were performed. Data are presented as means ± SD (n = 3) from one of three time-independent experiments with triplicate. Differences between PA alone and PA with API-2 were determined using the Student's *t*-test. \* *P* < 0.05. C: L6 cells were nucleofected with siRNA targeting Akt (siAkt) or negative control siRNA (N.C.). The cells were harvested after the indicated transfection times, and the total cell lysates obtained were subjected to Western blotting. D: L6 cells were nucleofected as in C and treated with 300 μM PA for 30 min after 48 h of transfection. <sup>3</sup>H-labeled 2-deoxy-D-glucose uptake assays were performed. Data are presented as means ± SD (n = 3) from one of three time-independent experiments with triplicate. Differences in PA effects between N.C.-transfected cells and siAkt-transfected cells were determined using the Student's *t*-test. \* *P* < 0.05.

AMPK but also Akt was stimulated rapidly by AICAR treatment in a time-dependent manner (Fig. 4A), which suggests that it is possible to stimulate Akt via AMPK activation in L6 cells. On the contrary, when we used AMPK inhibitor Compound C to suppress AMPK activity, we found Compound C could decrease PA-induced Akt phosphorylation (Fig. 4B) and glucose uptake (Fig. 4C). Moreover, when the myc-tagged AMPK dominant negative (AMPK-DN) plasmid was nucleofected into L6 cells

and AMPK-DN was expressed (Fig. 4D), PA-induced Akt phosphorylation (Fig. 4E) and glucose uptake (Fig. 4F) were also decreased. Furthermore, in the L6 cells transfected siRNA duplex mixture targeting AMPK catalytic subunits  $\alpha 1$  and  $\alpha 2$ , AMPK  $\alpha$  expression level was dramatically decreased as expected (Fig. 4G), and PA-stimulated Akt phosphorylation was also decreased (Fig. 4H), consistent with the inhibitor and AMPK-DN experiments. These data showed that PA-stimulated AMPK phosphorylation

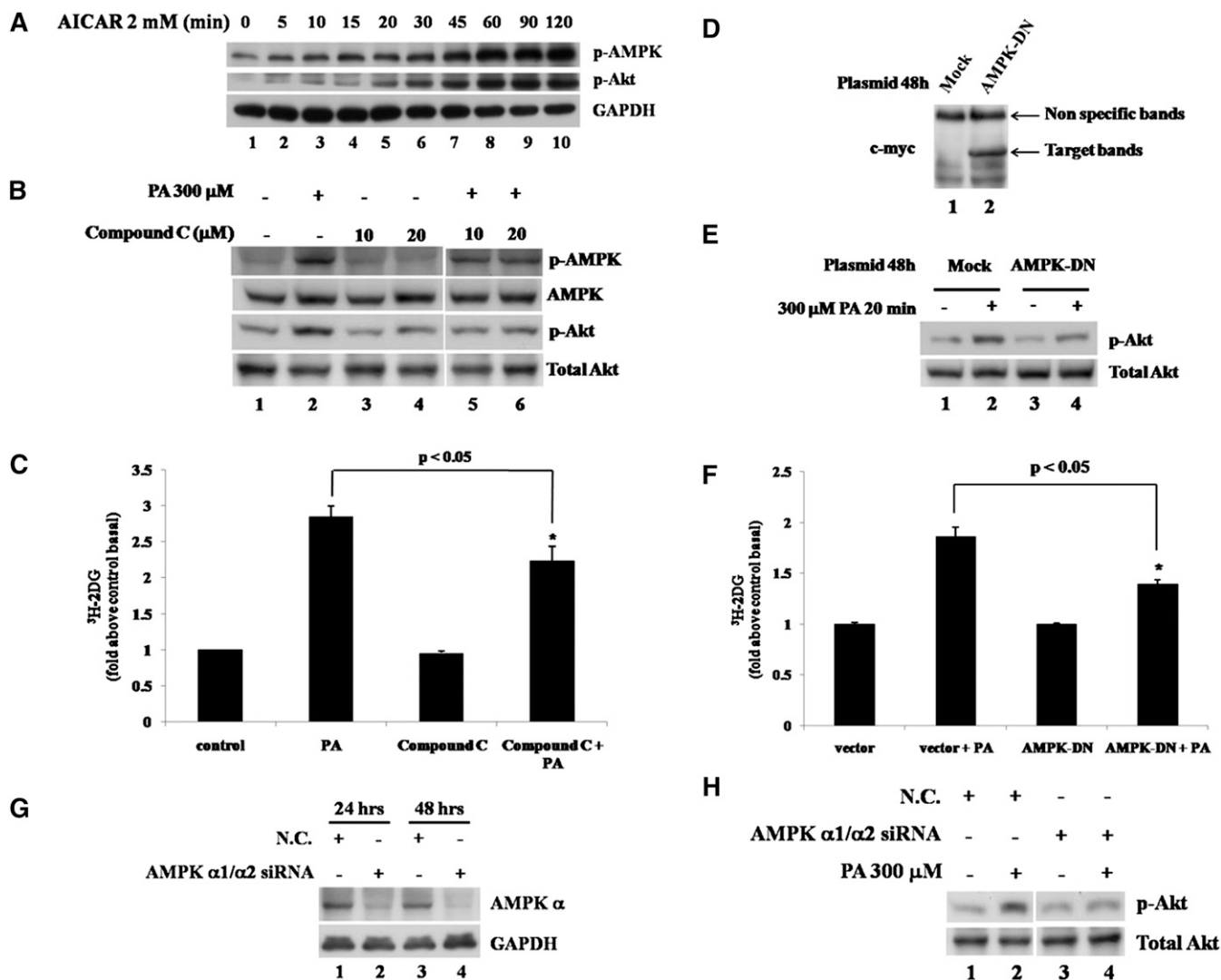


**Fig. 4.** AMPK is involved in palmitate-stimulated glucose uptake by regulating Akt activity. **A:** L6 cells were treated with 2 mM AICAR for the indicated times, and the total cell lysates obtained were subjected to Western blotting. **B:** L6 cells were pretreated with or without 10  $\mu$ M or 20  $\mu$ M Compound C for 1 h and then treated with 300  $\mu$ M PA alone or with 10  $\mu$ M or 20  $\mu$ M Compound C for 30 min. The total cell lysates were subjected to Western blotting. The images are from different lanes of the same gel. **C:** L6 cells were pretreated with or without 10  $\mu$ M Compound C for 1 h and then treated with 300  $\mu$ M PA alone or with 10  $\mu$ M Compound C for 30 min.  $^3$ H-labeled 2-deoxy-D-glucose uptake assays were performed. Data are presented as means  $\pm$  SD ( $n = 3$ ) from one of four time-independent experiments with triplicate. Differences between PA alone and PA with Compound C were determined using the Student's *t*-test. \*  $P < 0.05$ . **D:** L6 cells were nucleofected with pcDNA3.1 or AMPK-DN plasmids. After 48 h of transfection, cells were lysed and total proteins were obtained to analyze with anti-myc monoclonal antibody. **E:** L6 cells were transfected as in **D** and treated with or without 300  $\mu$ M PA for 30 min. Cells were lysed in 2 $\times$  SDS sample buffer, and total protein was subjected to Western blotting using the antibodies indicated. **F:** L6 cells were transfected and treated as in **E** and then subjected to  $^3$ H-labeled 2-deoxy-D-glucose uptake assays. Data are presented as means  $\pm$  SD ( $n = 3$ ) from one of three time-independent experiments with triplicate. Differences in PA effects between mock and AMPK-DN-transfected cells were determined using the Student's *t*-test. \*  $P < 0.05$ . **G:** L6 cells were nucleofected with siRNA duplex mixture targeting AMPK  $\alpha 1$  and  $\alpha 2$  or negative control siRNA (N.C.). The cells were harvested after the indicated transfection times and the total cell lysates obtained were subjected to Western blotting. **H:** L6 cells were nucleofected as in **G** and treated with or without 300  $\mu$ M PA for 30 min after 48 h of transfection. The cells were lysed, and the total proteins obtained were subjected to Western blotting. The images are from different lanes of the same gel.

might contribute to regulate Akt activity and was involved in PA-induced glucose uptake.

### PI3K mediates palmitate-stimulated glucose uptake by regulating AMPK and Akt activation

Because PI3K is upstream of Akt in the insulin signal pathway, we applied LY294002, a specific PI3K inhibitor, to the cells to determine whether PI3K functions in PA-

triggered glucose uptake. Unlike AMPK and Akt inhibitors that partially decreased glucose uptake, surprisingly, PI3K inhibitor could abolish it (Fig. 5A), suggesting that PI3K played an essential role in the cell response to PA. The Western blot results showed that PI3K inhibitor could reduce PA-induced AMPK activation (Fig. 5B) and block Akt phosphorylation (Fig. 5C). All the above data indicated that PA could rapidly trigger signal transduction by binding

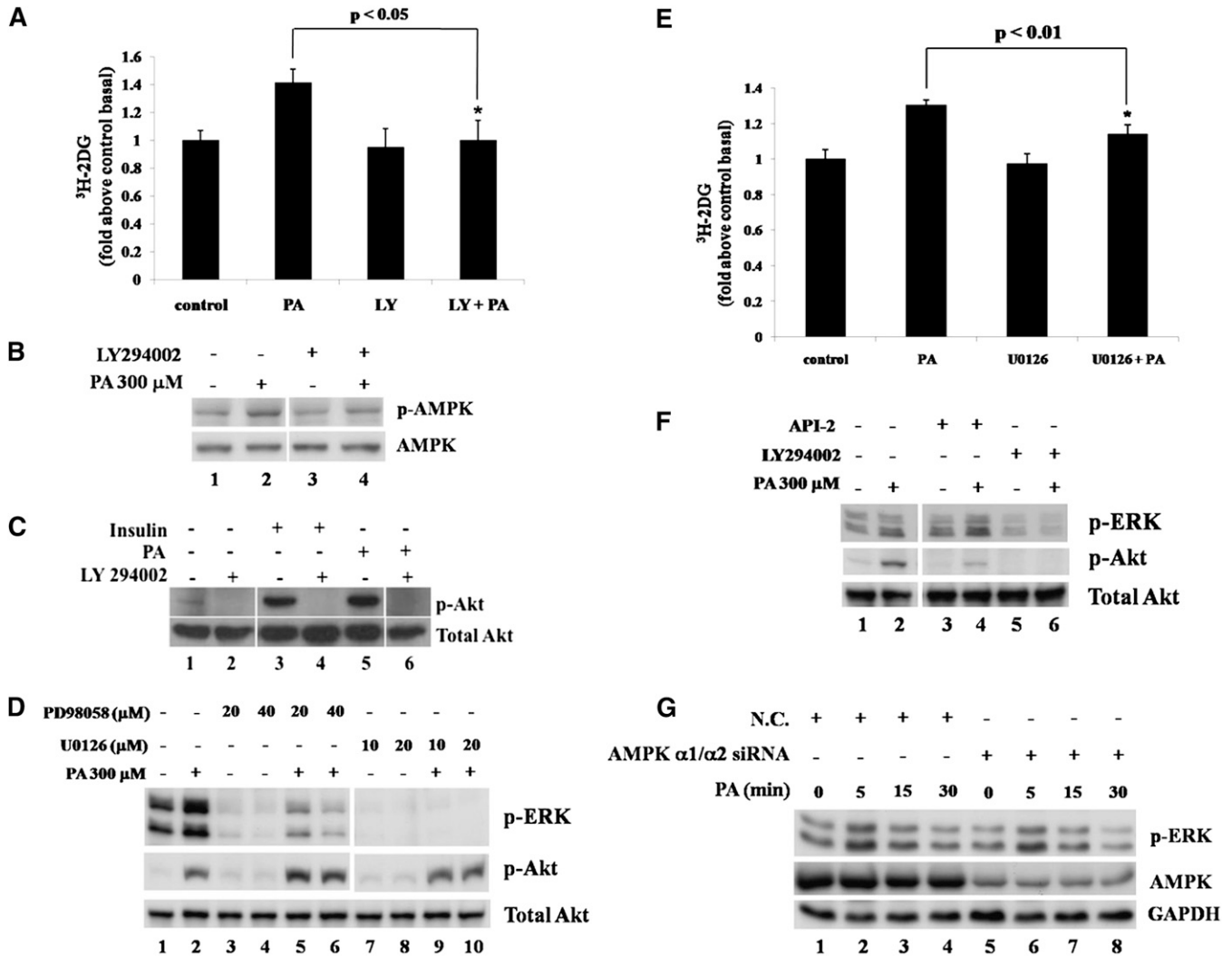


**Fig. 5.** PI3 kinase is involved in palmitate-stimulated glucose uptake, regulating ERK in an AMPK- and Akt-independent manner. **A:** L6 cells were pretreated with or without 50 μM LY294002 for 30 min and then with or without 300 μM PA alone or with inhibitor for 30 min. <sup>3</sup>H-labeled 2-deoxy-D-glucose uptake assays were performed. Data are presented as means ± SD (n = 3) from one of three time-independent experiments with triplicate. Differences between PA alone and PA with LY294002 were determined using the Student's *t*-test. \* *P* < 0.05. **B:** L6 cells were pretreated with or without 50 μM LY294002 for 30 min and then with or without 300 μM PA alone or with inhibitor for 15 min. Cells were lysed and total proteins were subjected to Western blotting. The images are from different lanes of the same gel. **C:** C2C12 cells were treated with 300 μM PA alone (lane 5) or with 50 μM LY294002 (LY) (lane 6) for 30 min, or 100 nM insulin with or without 50 μM LY294002 for 20 min. After treatment, cells were lysed and total protein was obtained and subjected to Western blotting. The images are from different lanes of the same gel. **D:** L6 cells were pretreated with or without PD98058 or U0126 at indicated concentrations for 90 min and then treated with 300 μM PA alone or combined with PD98058 or U0126 at the indicated concentrations for 10 min. Cell lysates were obtained and subjected to Western blotting. The images are from different lanes of the same gel. **E:** L6 cells were treated with or without 10 μM U0126 and 300 μM PA as in B and then subjected to <sup>3</sup>H-labeled 2-deoxy-D-glucose uptake assays. Data are presented as means ± SD (n = 3) from one of three time independent experiments with triplicate. Differences in PA effects between control cells and U0126 treated cells were determined using the Student's *t*-test. \* *P* < 0.01. **F:** L6 cells were pretreated with or without 2 μM API-2 or 50 μM LY294002 for 30 min and then treated with or without 300 μM PA alone or combined with above inhibitors for 10 min. Cell lysates were obtained and subjected to Western blotting. The images are from different lanes of the same gel. **G:** L6 cells were nucleofected with siRNA duplex mixture targeting AMPK α1 and α2 or negative control siRNA (N.C.) and treated with or without 300 μM PA for the indicated times after 48 h of transfection. The cells were lysed and the total proteins were obtained to subjected to Western blotting.

to cell plasma membrane and stimulate glucose uptake via activation of PI3K/AMPK/Akt cascade in skeletal muscle cells. The finding of the PI3K/AMPK/Akt pathway is consistent with recently published work by Youn et al (24).

#### Activation of ERK1/2 is involved in palmitate-stimulated glucose uptake in an AMPK and Akt-independent manner

Because blocking AMPK or Akt activity only partially decreased PA-induced glucose uptake, we investigated other possible pathways. The role of ERK1/2 in PA-stimulated signal transduction was examined by the MAPK/ERK kinase (MEK) 1/2 inhibitors PD98056 and U0126. Both inhibitors could decrease basal and PA-induced ERK1/2 phosphorylation, whereas U0126 worked more efficiently (Fig. 5D). When ERK1/2 activity was inhibited by U0126, PA-induced glucose uptake was reduced significantly (Fig. 5E). These data showed that PA-stimulated ERK1/2 phosphorylation may contribute to PA-induced glucose uptake. To determine the relationship between ERK1/2 and PI3K/AMPK/Akt pathways, first, PI3K inhibitor LY294002 was used. The results showed that PA-stimulated ERK1/2 phosphorylation was dramatically decreased (Fig. 5F, lane 6 vs. lane 2), suggesting PI3K was the upstream of ERK1/2 in PA-induced signal transduction. Second, in AMPK  $\alpha$ 1/ $\alpha$ 2 siRNA transfected cells, ERK1/2 phosphorylation was still increased normally as N.C. cells after PA treatment (Fig. 5G). Third, Akt inhibitor API-2 was used but did not affect PA-induced ERK1/2 phosphorylation (Fig. 5F lane 4 vs. lane 2), and finally, MEK1/2 inhibitors PD98056 and U0126 did not affect PA-induced Akt phosphorylation, either (Fig. 5D). These results suggest that in PA acute effects ERK1/2 was involved in PA-induced glucose uptake and regulated by PI3K but independent of AMPK and Akt.


## DISCUSSION

After meals, plasma free fatty acids respond to insulin (25), acylation stimulating protein (26), and other factors, decreasing rapidly to basal levels within 2 h. Thereafter, free fatty acids are released from adipocytes into the blood as an energy source. The plasma fatty acid concentration increases quickly and may reach about 400  $\mu$ M within several hours (10). Therefore, the free fatty acid concentration in blood varies considerably from hour to hour and forms a wave in every postprandial period. Under pathological conditions, plasma fatty acids also vary constantly but display different patterns; for example, obese nondiabetic humans have higher plasma fatty acid concentrations of 600–800  $\mu$ M compared with healthy subjects (27). However, how body tissues respond to the rapidly changing fatty acid levels remains unclear. Many studies have revealed that chronically elevated plasma free fatty acids play a critical role in the development of insulin resistance. Chronic fatty acid elevation may consist of many abnormal fatty acid cycles. Thus, studies on acute fatty acid effects and the cumulative effects of many acute fatty acid elevations may offer a different view for understanding the pathology of type 2 diabetes.

Results from previous studies on adipocytes indicate that short-term treatment with fatty acids increases basal glucose uptake (13, 28, 29). Some reports provide evidence that fatty acids share at least part of a common pathway with insulin (13), whereas other reports indicate the involvement of GLUT1 but not GLUT4 (30); a consistent picture of the mechanisms involved has not yet emerged. More importantly, less is known about the situation in skeletal muscle cells. Here, we studied the short-term effects of PA in skeletal muscle cell lines and tissues, and results indicate that PA-stimulated glucose uptake occurs via activation of the PI3K/AMPK/Akt and PI3K/ERK1/2 pathways to lead GLUT4 translocation (Fig. 6).

Insulin receptor autophosphorylation has been observed after acute PA treatment in isolated adipocytes (13), and in our work, we found that plasma membrane-bound PA was sufficient to induce Akt phosphorylation, indicating that PA might interact with some protein(s) on the plasma membrane to trigger the signal. However, the identity of this protein(s) still needs to be determined.

Phosphorylation of Akt was stimulated only when the concentrations of PA reached a certain level (at or above 200  $\mu$ M in C2C12 cells). Thus, we concluded that phosphorylation of Akt may require high concentrations of fatty acids under physiological situations. According to our results, Akt phosphorylation was detectable after fatty acid treatments of up to 3 h (Fig. 2A), and when fatty acids were withdrawn, the Akt phosphorylation signal disappeared after 3 h in C2C12 cells (data not shown), suggesting that fatty acid-induced phosphorylation and dephosphorylation of Akt can be completed within one fatty acid cycle. Many abnormal fatty acid cycles might contribute to the development of insulin resistance via the desensitization of Akt.

The most significant implication of the above results is that PA can play two opposing roles in skeletal muscle. On one hand, under chronic treatment, it can inhibit insulin-induced glucose uptake by blocking Akt phosphorylation, and on the other hand, when cells are exposed to PA for a short time, it can enhance glucose uptake by activating Akt. This Yin-Yang balance of PA in skeletal muscle must be physiologically significant and needs to be investigated further. 

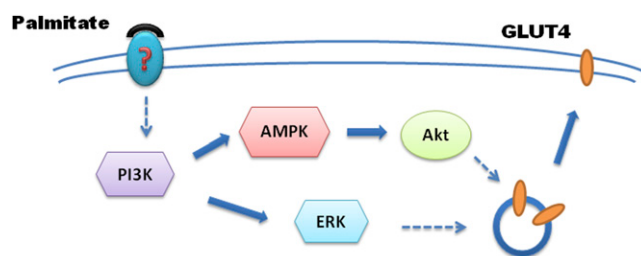


**Fig. 6.** Pathways PI3K/AMPK/Akt and PI3K/ERK1/2 in mediating palmitate-stimulated glucose uptake. In response to plasma membrane-bound palmitate, signal is transduced by activation of PI3K/AMPK/Akt and PI3K/ERK1/2, which in turn leads GLUT4 translocation to plasma membrane and glucose uptake in skeletal muscle cells.



The authors thank Drs. John Zehmer and Joy Fleming for their critical reading and useful suggestions. The authors also want to thank Drs. Huina Zhang and Shuyan Zhang for their administrative support. We are grateful to Dr. David Carling for AMPK-DN construct.

## REFERENCES

1. Savage, D. B., K. F. Petersen, and G. I. Shulman. 2007. Disordered lipid metabolism and the pathogenesis of insulin resistance. *Physiol. Rev.* **87**: 507–526.
2. McGarry, J. D. 1992. What if Minkowski had been ageusic? An alternative angle on diabetes. *Science*. **258**: 766–835.
3. DeFronzo, R. A., E. Jacot, E. Jequier, E. Maeder, J. Wahren, and J. P. Felber. 1981. The effect of insulin on the disposal of intravenous glucose. Results from indirect calorimetry and hepatic and femoral venous catheterization. *Diabetes*. **30**: 1000–1006.
4. Shulman, G. I., D. L. Rothman, T. Jue, P. Stein, R. A. DeFronzo, and R. G. Shulman. 1990. Quantitation of muscle glycogen synthesis in normal subjects and subjects with non-insulin-dependent diabetes by <sup>13</sup>C nuclear magnetic resonance spectroscopy. *N. Engl. J. Med.* **322**: 223–230.
5. Martin, S., and R. G. Parton. 2006. Lipid droplets: a unified view of a dynamic organelle. *Nat. Rev. Mol. Cell Biol.* **7**: 373–380.
6. Zhang, S., Y. Du, Y. Wang, and P. Liu. 2010. Lipid droplet—a cellular organelle for lipid metabolism. *Acta Biophysica Sinica*. **26**: 97–105.
7. Pan, D. A., S. Lillioja, A. D. Kriketos, M. R. Milner, L. A. Baur, C. Bogardus, A. B. Jenkins, and L. H. Storlien. 1997. Skeletal muscle triglyceride levels are inversely related to insulin action. *Diabetes*. **46**: 983–990.
8. Manco, M., G. Mingrone, A. V. Greco, E. Capristo, D. Gniuli, A. De Gaetano, and G. Gasbarrini. 2000. Insulin resistance directly correlates with increased saturated fatty acids in skeletal muscle triglycerides. *Metabolism*. **49**: 220–223.
9. Roden, M. 2005. Muscle triglycerides and mitochondrial function: possible mechanisms for the development of type 2 diabetes. *Int J Obes (Lond)*. **29(Suppl 2)**: S111–S115.
10. Singer, P., W. Godicke, S. Voigt, I. Hajdu, and M. Weiss. 1985. Postprandial hyperinsulinemia in patients with mild essential hypertension. *Hypertension*. **7**: 182–187.
11. Coppack, S. W., R. M. Fisher, G. F. Gibbons, S. M. Humphreys, M. J. McDonough, J. L. Potts, and K. N. Frayn. 1990. Postprandial substrate deposition in human forearm and adipose tissues in vivo. *Clin. Sci. (Lond.)*. **79**: 339–386.
12. Eason, R. C., H. E. Archer, S. Akhtar, and C. J. Bailey. 2002. Lipoic acid increases glucose uptake by skeletal muscles of obese-diabetic ob/ob mice. *Diabetes Obes. Metab.* **4**: 29–35.
13. Hardy, R. W., J. H. Ladenson, E. J. Henriksen, J. O. Holloszy, and J. M. McDonald. 1991. Palmitate stimulates glucose transport in rat adipocytes by a mechanism involving translocation of the insulin sensitive glucose transporter (GLUT4). *Biochem. Biophys. Res. Commun.* **177**: 343–351.
14. Liu, P., Y. Ying, Y. Zhao, D. I. Mundy, M. Zhu, and R. G. Anderson. 2004. Chinese hamster ovary K2 cell lipid droplets appear to be metabolic organelles involved in membrane traffic. *J. Biol. Chem.* **279**: 3787–3878.
15. Katome, T., T. Obata, R. Matsushima, N. Masuyama, L. C. Cantley, Y. Gotoh, K. Kishi, H. Shiota, and Y. Ebina. 2003. Use of RNA interference-mediated gene silencing and adenoviral overexpression to elucidate the roles of AKT/protein kinase B isoforms in insulin actions. *J. Biol. Chem.* **278**: 28312–28334.
16. Konrad, D., A. Rudich, P. J. Bilan, N. Patel, C. Richardson, L. A. Witters, and A. Klip. 2005. Troglitazone causes acute mitochondrial membrane depolarisation and an AMPK-mediated increase in glucose phosphorylation in muscle cells. *Diabetologia*. **48**: 954–1019.
17. Wang, Q., Z. Khayat, K. Kishi, Y. Ebina, and A. Klip. 1998. GLUT4 translocation by insulin in intact muscle cells: detection by a fast and quantitative assay. *FEBS Lett.* **427**: 193–199.
18. Li, W. P., P. Liu, B. K. Pilcher, and R. G. Anderson. 2001. Cell-specific targeting of caveolin-1 to caveolae, secretory vesicles, cytoplasm or mitochondria. *J. Cell Sci.* **114**: 1397–1408.
19. Fediuc, S., M. P. Gaidhu, and R. B. Ceddia. 2006. Regulation of AMP-activated protein kinase and acetyl-CoA carboxylase phosphorylation by palmitate in skeletal muscle cells. *J. Lipid Res.* **47**: 412–431.
20. Pimenta, A. S., M. P. Gaidhu, S. Habib, M. So, S. Fediuc, M. Mirpourian, M. Musheev, R. Curi, and R. B. Ceddia. 2008. Prolonged exposure to palmitate impairs fatty acid oxidation despite activation of AMP-activated protein kinase in skeletal muscle cells. *J. Cell. Physiol.* **217**: 478–562.
21. Ouchi, N., H. Kobayashi, S. Kihara, M. Kumada, K. Sato, T. Inoue, T. Funahashi, and K. Walsh. 2004. Adiponectin stimulates angiogenesis by promoting cross-talk between AMP-activated protein kinase and Akt signaling in endothelial cells. *J. Biol. Chem.* **279**: 1304–1312.
22. Yamazaki, K., T. Hamazaki, S. Yano, T. Funada, and F. Ibuki. 1991. Changes in fatty acid composition in rat blood and organs after infusion of docosahexaenoic acid ethyl ester. *Am. J. Clin. Nutr.* **53**: 620–626.
23. Yang, L., H. C. Dan, M. Sun, Q. Liu, X. M. Sun, R. I. Feldman, A. D. Hamilton, M. Polokoff, S. V. Nicosia, M. Herlyn, et al. 2004. Akt/protein kinase B signaling inhibitor-2, a selective small molecule inhibitor of Akt signaling with antitumor activity in cancer cells overexpressing Akt. *Cancer Res.* **64**: 4394–4402.
24. Youn, J. Y., T. Wang, and H. Cai. 2009. An ezrin/calpain/PI3K/AMPK/eNOSs1179 signaling cascade mediating VEGF-dependent endothelial nitric oxide production. *Circ. Res.* **104**: 50–58.
25. Campbell, P. J., M. G. Carlson, J. O. Hill, and N. Nurjhan. 1992. Regulation of free fatty acid metabolism by insulin in humans: role of lipolysis and reesterification. *Am. J. Physiol.* **263**: E1063–E1071.
26. Saleh, J., L. K. Summers, K. Cianflone, B. A. Fielding, A. D. Sniderman, and K. N. Frayn. 1998. Coordinated release of acylation stimulating protein (ASP) and triacylglycerol clearance by human adipose tissue in vivo in the postprandial period. *J. Lipid Res.* **39**: 884–974.
27. Paquot, N., A. J. Scheen, M. Dirlwanger, P. J. Lefebvre, and L. Tappy. 2002. Hepatic insulin resistance in obese non-diabetic subjects and in type 2 diabetic patients. *Obes. Res.* **10**: 129–162.
28. Nugent, C., J. B. Prins, J. P. Whitehead, J. M. Wentworth, V. K. Chatterjee, and S. O’Rahilly. 2001. Arachidonic acid stimulates glucose uptake in 3T3-L1 adipocytes by increasing GLUT1 and GLUT4 levels at the plasma membrane. Evidence for involvement of lipoxygenase metabolites and peroxisome proliferator-activated receptor gamma. *J. Biol. Chem.* **276**: 9149–9205.
29. Hunnicutt, J. W., R. W. Hardy, J. Williford, and J. M. McDonald. 1994. Saturated fatty acid-induced insulin resistance in rat adipocytes. *Diabetes*. **43**: 540–544.
30. Fong, J. C., C. C. Chen, D. Liu, S. P. Chai, M. S. Tu, and K. Y. Chu. 1996. Arachidonic acid stimulates the intrinsic activity of ubiquitous glucose transporter (GLUT1) in 3T3-L1 adipocytes by a protein kinase C-independent mechanism. *Cell. Signal.* **8**: 179–261.